Behavior of Water in the Hydrophobic Zeolite Silicalite at Different Temperatures. A Molecular Dynamics Study

Pierfranco Demontis, Giovanna Stara, and Giuseppe B. Suffritti*

Dipartimento di Chimica, Università di Sassari and Consorzio Interuniversitario Nazionale per la Scienza e Tecnologia dei Materiali (INSTM), Unità di ricerca di Sassari,Via Vienna, 2, 07100 Sassari, Italy

Received: January 23, 2003

Classical molecular dynamics simulations of water adsorbed in silicalite, a hydrophobic all-silica zeolite, were performed at different temperatures in the range 100−580 K, to explore possible phase transitions and to compare the behavior of adsorbed water with that of bulk water or water confined in nanopores of different geometry. We used a potential model including full flexibility both of water molecules and of the silicate framework. The results show an unexpected complexity. At very low temperatures (below 225 K), water appears to be mostly in form of amorphous solidlike clusters among which a slow molecule interchange occurs, giving rise to a single-file like diffusion on the time scale of our simulations. At intermediate temperatures, in the approximate range of 225−350 K, the behavior of water is almost liquidlike, whereas at higher temperatures, there are evidences of a vaporlike features, in agreement with the suggestions of previous theoretical and experimental works. This behavior is discussed by considering, among others, the average distribution of water in the channels, the size and lifetime of the hydrogen bonded clusters, and the water−water interaction energy. The results are compared with the available experimental data, previous simulations, and statistical mechanical studies.

Introduction

The behavior of water in confining media has recently received a renewed interest, both from experimental and theoretical viewpoint. These media may be of a biological nature, like cellular membranes or enzyme channels, as well as an inorganic one. Some examples of inorganic microporous materials adsorbing water are carbon nanotubes, porous silica glasses and zeolites, or molecular sieves, which are important for their industrial and environmental applications. There is much experimental and theoretical evidence indicating that the properties of water, when confined in nanopores, are different from those of common bulk water.[1,2] For instance, the experimental evidence of possible phase transitions of supercritical liquid water at low temperatures has been looked for in hydrated phyllosilicates,[3−6] where the confinement would prevent nucleation, whereas new statistical models have been developed for studying the phases of water-like liquids in nanoporous media.[7−9] Among the different approaches, the molecular dynamics (MD) simulation technique seems to be very promising in order to gain a better microscopic description for the behavior of water in porous materials. Recent examples are the study of the phase transitions of water in slit pores[10] and the analysis of structure of water confined in porous Vycor glass.[11]

In the field of zeolites, a class of nanoporous aluminosilicates of outstanding practical interest, after a pioneering study performed in this laboratory on the natural zeolite natrolite,[12] a series MD simulations of water adsorbed in the zeolite ferrierite were carried out by Leherte et al.,[13−18] showing that the inclusion of long-range Coulombic interactions is mandatory for systems including water. Other minor studies were reviewed in 1997 in ref 19. More recently, Faux et al.[21,22] investigated hydrated zeolite A. Previous simulations of water in silicalite are discussed below.

In the present work, MD simulations of water in silicalite[23,24] extended to the nanosecond scale and to different temperatures in the range of 100−580 K are illustrated. Silicalite is the all-silica analogue of the synthetic zeolite catalyst ZSM-5. Therefore, the cations usually located in the channels that compensate for the extra charge due to the Al/Si substitutions are not present. In other words, the behavior of water is dominated by the hydrogen bonding interactions and the role of the host zeolite resides essentially in the steric hindrance and in the shape of the channels. Its framework structure comprises two different channel systems; each defined by ten-membered rings. Straight channels with an elliptical kinetic cross section of approximately 5.7−5.2 Å are parallel to the crystallographic axis *b*, and sinusoidal channels with nearly circular cross section of 5.4 Å run along the crystallographic axis *a*. The resulting intersections are elongated cavities up to 9 Å in diameter. This zeolite is of special interest because, among others, it shows a hydrophobic character: the water−water interactions are stronger than the interactions of water molecules with the zeolite framework. Hydrophobic zeolites are important for some possible environmental applications, for instance, the remediation of chlorinated volatile organic compounds in drinking water.[25] A theoretical interest of these systems is connected with the above-mentioned studies about the behavior of nanoconfined water,[7−9] which has been recently extended to the hydrophobic carbon nanotubes.[26−29]

As the zeolite means "boiling stone" because of the great hydrophilicity of most natural zeolites, which expel water vapor when heated, an "hydrophobic zeolite" could sound as an oxymoron. However, the term "zeolite" has been recently extended to aluminum-free porous silicates (as well as to any crystal of similar structure, as, for example, alumino- or gallophosphates) and some of them are hydrophobic. Indeed,

* To whom correspondence should be addressed. E-mail: pino@uniss.it.

10.1021/jp0300849 CCC: $25.00
Published on Web 04/12/2003

hydrophobic zeolites are included in the title of a paper recently presented to the *Comptes Rendus de Physique* by Pierre-Gilles de Gennes.[30]

Unfortunately, just because silicalite is hydrophobic, the experimental studies of adsorption[31−35] and diffusion[36−38] of adsorbed water are not abundant, may be affected by large uncertainties, or deserve a special treatment because they are influenced by the aluminum content of the real crystal or by defects of the crystal lattice, which are almost never negligible.

Although most of the available experimental data were obtained at room temperature, we performed the simulations of water in silicalite at different temperatures, in the range 100−580 K, to explore possible different aggregation states and to compare the behavior of adsorbed water with that of bulk water, or water confined in nanopores of different geometry. We used a potential model including full flexibility both of water molecules and of the silicate framework, because we were interested in the details of the adsorbed water dynamics and this is closely related to the vibrations of the alluminosilicate framework, as discussed for different systems in a series of papers.[19,39−42]

The results show an unexpected complexity. At very low temperatures (below 200 K), water appears to be mostly in the form of amorphous solidlike clusters among which a slow molecule interchange occurs, giving rise to a single-file like diffusion, on the time scale of our simulations. At intermediate temperatures, in the approximate range of 200−350 K, the behavior of water is almost liquidlike, whereas at higher temperatures, there are evidences of a vaporlike features, in agreement with the suggestions of theoretical[9] and experimental[35] studies.

These findings might be compared with the properties of supercooled liquid water, which are not yet completely explored and understood.[3−6,43] Indeed, ordinary and supercooled liquid water is a "fragile" liquid[44,45] (shortly, its dynamical properties do not follow the Arrhenius dependence on temperature), but the interpretation of its behavior at temperatures between 136 and 158 K (for which some dynamical properties, as diffusivity, follow the Arrhenius trend) is under discussion.[45] Previous recent simulation studies of water in silicalite were carried out by Bussai et al.[38,46,47] Use was made of water−framework potential functions derived by fitting ab initio energy calculations.[47,48] These authors kept the framework fixed while retaining the water flexibility.[38,47] The simulations were performed at room temperature and at 393 K, to compare the diffusion coefficients with the experimental ones. The agreement was reasonable, but the behavior of water at low temperature was not explored.

Model and Calculations

The simulation of water in a partially ionic material like zeolites requires potential model including long-range electrostatic forces, and able to reproduce the hydrophobic character of all-silica zeolites. Moreover, because water is often used as a probe of the charge distribution in the channels of zeolites by monitoring the geometry deformation of the molecules and their vibrational frequency shifts, it is preferable to use a model including also their flexibility and the correct response to the electrostatic interactions.

Accordingly, an electric field dependent potential was developed in this laboratory,[49] yielding a satisfactory description of bulk water and of structural and vibrational properties of water adsorbed in zeolites. However, the resulting empirical potential functions that had been used for representing zeolite−water interactions in ref 49 had to be refined in order to fit better the properties of a series of hydrated zeolites, including bikitaite,[50] natrolite,[51] and scolecite.[52]

TABLE 1: Parameters for the Interactions between an Oxygen Atom of the Zeolitic Framework (O) and an Oxygen Atom (O_w) or a Hydrogen Atom (H_w) of Water [eqs 1 and 2][a]

parameters	A	B	C
$O-O_w$	8.36×10^5	3100	209
$O-H_w$	2090	179.9	
charges	q_O	q_{O_w}	q_{H_w}
	−1.0	−0.65966	0.32983

[a] Energies are in kJ/mol, and distances are in Å. Charges are in units of *e*.

As in our previous paper,[49] water was assumed to interact with Si and Al atoms via a Coulomb potential only, and the potential functions between the oxygen atoms of the framework and the oxygen or hydrogen atoms of water were derived from a simplified form of the corresponding O−O and O−H ones for water−water interactions.

The potentials for interactions between an oxygen atom of the zeolite framework (O) and an oxygen (O_w) or an hydrogen (H_w) atom of the water molecule were represented by

$$V_{OO_w} = \frac{1}{4\pi\epsilon_0}\frac{q_O q_{O_w}}{r} + \frac{A}{r^{12}} - \frac{B}{r^6} + \frac{C}{r^4} \quad (1)$$

$$V_{OH_w} = \frac{1}{4\pi\epsilon_0}\frac{q_O q_{H_w}}{r} + \frac{A}{r^7} - \frac{B}{r^4} \quad (2)$$

and the values of the refined parameters are reported in Table 1. An empirical model for simulating flexible zeolite framework developed in this laboratory[53] was used. This model includes electrostatic interactions between particles, besides Morse potentials for representing Si−O bonds and third-order polynomials for the O−O and Si−Si first-neighbors interactions. It was fitted to structural and vibrational properties of silicalite and of anhydrous Na, Ca, and NaCA A zeolites. The analytical form and the parameters are reported in the Appendix. The evaluation of the Coulomb energy is very computer time demanding, so that it was performed using the efficient method recently proposed by Wolf et al.[54] and extended in our laboratory to complex systems.[55]

In the present study, the polarizability of the water molecules was not taken into account explicitly because it is in part included in the adopted electric field dependent potential[49] and the lack of exchangeable ions in silicalite (and therefore of local strong electric fields) should make the influence of polarization small or negligible. On the other hand, the adopted potential, which was optimized for liquid water, proved to be reasonably accurate also for the water dimer and, therefore, for water−water interactions, the most important ones in the system under consideration.

Standard MD simulations with periodic boundary conditions and in the microcanonical ensemble were performed for a system consisting in $1 \times 1 \times 2$ unit cells of silicalite loaded with 16 water molecules (8 molecules per unit cell). One crystallographic cell contains 288 atoms (96 Si and 192 O). Silicalite shows a reversible phase transition at about 340 K and exhibits monoclinic symmetry ($P2_1/n11$ space group) below and orthorhombic (*Pnma* space group) above the transition temperature. Both structures were accurately determined by van Koningsveld et al.[23,24] The cell parameters are very similar for the two structures, and the deviation from orthogonality of axes in monoclinic

structure is only 0.67°. Moreover, it is well-known that zeolites show a negligible thermal expansion, so that we choose to adopt for all simulations the simpler othorhombic unit cell, as the phase transition is practically uninfluential for the study of the diffusive processes. Two unit cells superimposed along *c* yielded an orthorhombic simulation box of $2.0022 \times 1.9899 \times 2.6766$ nm^3 containing 576 framework atoms and 16 water molecules. The number of water molecules corresponds to the maximum loading of the samples used for experimental measurements of both diffusion coefficient and adsorption heat.

The simulations were carried out in the *NVE* (microcanonical) ensemble at a series of temperatures in the range (100−580 K) to check the behavior of the water molecules. The MD runs lasted, after equilibration, 7 ns for the simulation at 100 K, 4 ns in the intermediate range (130, 160, and 200 K), and at least 3 ns in the higher temperature range (225 250, 300, 350, 400, 450, and 580 K). These relatively long simulations were necessary in order to ensure a good statistics not only in consideration of the small number of the adsorbed water molecules but also because the intermolecular interactions are stronger than in the case of nonpolar sorbates, hindering the sampling of all possible configurations. The Monte Carlo (MC) simulation method was discarded because we were interested in the detailed dynamics of the system. It could be used in the grand canonical MC form to study possible phase transitions of adsorbed water, but this is out of the scope of this study.

The considered number of atoms and the length of the simulations are far beyond any actual possible use of the so-called first principles MD, as the Car-Parrinello method,[43] which actually can hardly handle systems containing some hundreds of atoms and simulations a few tens of picosecond long.

A time step of 0.5 fs was used, ensuring good total energy conservation and mean temperatures within a few degrees around the nominal ones. This value, which could be considered exceedingly small, is the same usually adopted for MD simulations of water, even in the case of rigid molecules (see for instance ref 10).

From the simulations several quantities and functions able to help in understanding the behavior of water were evaluated.[19] Among structural properties, the water−water and water−zeolite radial distribution functions and three-dimensional distributions of the molecules in the channels were considered. Average interaction energies between water molecules and between water and the zeolite framework, as well as adsorption heats,[57] were stored separately. The mean lifetime of the clusters[58] of water molecules was evaluated. As for the diffusivity, the mean square displacement (MSD) computed as a function of time was analyzed by using log−log plots[59] in order to establish the power law of the time dependence of MSD. Indeed, if it is assumed that the MSD depends on time as

$$\langle \mathbf{r}^2 \rangle = Ct^{\alpha} \tag{3}$$

where C is constant, then α is given by the slope of the logarithm of MSD vs the logarithm of time. If $\alpha = 1$ ("normal" diffusion), the well-known Einstein formula[19] can be used to estimate the diffusion coefficient. In the other cases, the diffusivity can be characterized directly from the MSD trend. However, when molecules cannot pass each other in the channels, single-file diffusion regime[60−62] is observed entailing, for long but not infinite time,[63] a value $\alpha = 0.5$ and the MSD is given by

$$\langle \mathbf{r}^2 \rangle = 2F\sqrt{t} \tag{4}$$

where F is the mobility factor of single-file diffusion.

Results and Discussion

Comparison with Experimental Data. The behavior of water in silicalite was studied experimentally by measuring the adsorption heat and by NMR spectroscopy allowing to estimate the mobility of the sorbed molecules,[64,65] where, among others, the formation of water molecule clusters was invoked to explain the trend of the spectra at temperatures lower than 265 K and their diffusion coefficients (using in particular the pulsed gradient field, PGF, technique).[36−38] The NMR experiments were carried over in the temperature range of 220−330 K, whereas the diffusion coefficients were estimated at room temperature and at 393 K.

The values of the diffusion coefficients reported in the different studies are different because, due to the hydrophobicity of silicalite, water enters in its channels in small quantities, and the corresponding signals are weak. Moreover, depending on temperature, the measures are made difficult by the presence of water in liquid or vapor form on the surface of the crystallites or in the interstitial spaces among them, respectively. Another source of uncertainty, affecting also the adsorption heats, is the presence of defects in the framework, as this material cannot be easily synthesized in ultrapure SiO_2 form and contains a small quantity of Al atoms, or a non-negligible number of Si−O−Si bridges are open to form silanol groups. Therefore, on the internal surfaces of silicalite, there are charge compensating cations (H^+ or metallic) or polar groups to which water molecules stick more tightly than to the all-silica surfaces.

When evaluating the adsorption heat, the problem can be overcome by considering its limiting value for high water loading, if its measure depending on the number of adsorbed molecules per unit cell is available, as in ref 34. Indeed, the adsorption heat usually decreases with loading, because a strongly bounded cluster of water molecules (approximately four in H-ZSM-5)[34] is formed around each H^+, metallic cation, or silanol group, and the other added molecules are less and less bound to that cluster. The adsorption heat for the *n*th added molecule per unit cell q_n can be evaluated from the average integrated value given by the experimental curve by considering that

$$q_n = nQ_n - (n-1)Q_{n-1} \tag{5}$$

where $Q_n = 1/n\sum_{k=1}^{n} q_k$ is the average integral adsorption heat for a loading with n molecules.

Unfortunately, this treatment is not very accurate, but it could be applied to the data of ref 34, obtaining a q_n that for $n > 7$ becomes practically constant with a value of 32 ± 5 kJ/mol. The relatively large error includes both the estimated uncertainties in reading the fitting experimental curve and the scatter of the reported experimental points. Other more recent experiments[35] show apparently more accurate data but in a partially different range of water loading, with the adsorption heat larger than the one reported in ref 34 and slightly *increasing* for higher water concentration, possibly due to the attraction between water molecules. This result is not incompatible with the data of ref 34. Figure 8 of this paper shows a similar trend in the same water loading interval, although it is obscured by a decreasing fitting line.

Other previous experimental values of adsorption heat, all at room temperature, are available[31−33] and are compared in Table 2 with the computed result (32.5 kJ/mol). The agreement is satisfactory, although the computed value seems slightly too low, but be remind that it was fitted to the properties of several zeolites. It was verified that a small adjustment of the parameters

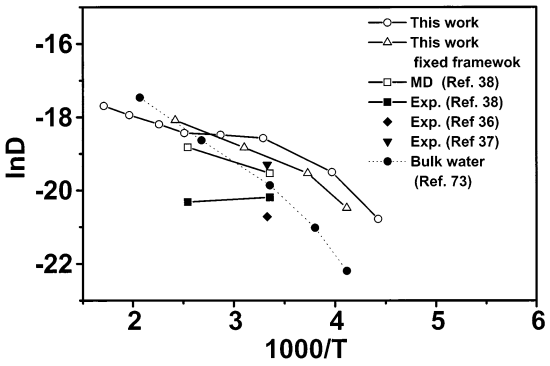

Figure 1. Arrhenius plot of diffusion coefficients of water in silicalite evaluated from the simulations described in this work using both the flexible and fixed framework models, along with calculated and experimental results from ref 24, and experimental values from refs 22 and 23. For comparison, experimental diffusion coefficients of bulk water (ref 56) are also reported. Error bars of the diffusion coefficients computed in this work have about the same dimensions of the symbols and are not shown.

TABLE 2: Experimental and Computed Adsorption Heats and Diffusion Coefficients[a]

	ΔH (kJ/mol)		D (10^{-9} m^2s^{-1})		
T (K)	this work	exp	this work	MD	PFG NMR
298	32.5	25.1[b]	8.6	3.3[c]	1.7 [c]
		34.3−50.6[d]	6.6[e]		4.0[f]
		40.2[g]			1.0[h]
		32.5[i]			
		38.0[j]			
393	30.0		10.0	6.7[c]	1.5[c]
			15.0[e]		

[a] The relative standard error of the values computed in this work does not exceeds 10%. [b] Reference 31. [c] Reference 38. [d] Reference 32. [e] Fixed framework model. [f] Reference 37. [g] Reference 33. [h] Reference 36. [i] Reference 34. [j] Reference 35.

could yield a better fit of the average experimental data without affecting the other computed quantities significantly.

We recall that adsorption heat can be evaluated from the simulations, for low dilution, by[57]

$$Q = -\langle U_{gz}\rangle - \langle U_{gz}\rangle + RT \qquad (6)$$

where $\langle U_{gz}\rangle$ and $\langle U_{gg}\rangle$ are the guest molecule−zeolite and guest molecule−guest molecule average energies, respectively, *R* is the molar gas constant and *T* is the temperature.

It is interesting to remark that both experimental and computed adsorption heats are smaller than the sublimation heat of bulk water at room temperature (43.5 kJ/mol).[66]

Also the values of the diffusion coefficient (*D*) reported in the experimental studies deserve some comments. To our knowledge, all of them were obtained by the PGF NMR technique and by the same Laboratory at different times.[36−38] At room temperature, they are approximately in the range 1−4 × 10^{-9} m^2 s^{-1}, which, interestingly, includes the diffusion coefficient of bulk liquid water (2.4 × 10^{-9} m^2 s^{-1}).[67] The most recent value (1.7 × 10^{-9} m^2 s^{-1} at 298 K)[38] is slightly *higher* than the diffusion coefficient measured with the same experimental setting at 393 K (1.5 × 10^{-9} m^2 s^{-1}). The last temperature was chosen in order to avoid the presence of liquid water on the external surface of the crystallites, which could affect the accuracy. This unexpected decrease, which could be caused by an enhanced rotational motion of the water molecules, thus enlarging their effective kinetic radius,[68] is not reproduced by the simulation results reported in the same paper. On the contrary, in our simulations from 300 to 450 K, the diffusion coefficients become almost constant (see Figure 1), but for higher temperatures, they increase again, probably because, once a free rotation regime is established, only the translational barrier to diffusion remains into play.

Moreover, the experimental values of the diffusion coefficient can be affected by an even small amount of Al or of silanol groups because of the opening of Si−O−Si bridges the framework, taking into account the low water loading in silicalite. Indeed, if up to four water molecules stick to a charge compensating cation or to the silanol group with a bonding energy much larger than the adsorption heat for all-silica silicalite,[34] they do not diffuse at ordinary temperature. Thus, the resulting experimental value of *D*, which is averaged over all water molecules, is lower than the real diffusion coefficient for the all-silica zeolite. These considerations may be confirmed, for instance by the results reported in ref 36, where the Arrhenius plot of the diffusion coefficient of water in Na- and H-ZSM-5 is shown. It appears that the diffusion coefficients are different but the activation energy is practically the same, despite the different bonding energy of water with the two cations. This means that the activation energy is related with the mobile molecules only, and the different values of the diffusion coefficients can be explained by the different number of molecules bound to the cations, which do not diffuse, and by the different steric hindrance of the hydration clusters. However, it is not easy to predict a priori how much the measured diffusion coefficient is affected by this phenomenon in a particular sample.

The diffusion coefficients evaluated in this work are reported in Table 2 along with the experimental values and the results of previous simulations. The agreement is reasonably good, in view of the above-reported considerations. The uncertainty of the computed values was estimated by comparing the results of different portions of the same run, as it was found in general smaller that 10%.

The use of a fixed framework for MD simulations of silicalite, as assumed by Bussai et al.,[38] deserves some comments. In general, this approximation has been the object of a lively debate,[19] which is still active.[39−42] Without entering in technical details, previous studies on this effect, based on a wealth of MD simulations,[19,41,70−72] have permitted to draw the following conclusions:

(i) Lattice vibrations provide an efficient heat bath in any case.[19]

(ii) At infinite dilution (one sorbate per simulation box) when the energy barrier to diffusion is low, the influence of the lattice vibration is relatively small.[19,41,72] Otherwise, if the transition state involves the crossing of a window whose diameter is smaller than the sorbate diameter, the lattice vibration effect can be large (see, for example, ref 70). However, when the barrier is high, but in the transition state the sorbate is not close to a channel wall (like for example benzene in NaY zeolite[71]) the influence of lattice vibration is again small.

(iii) At finite loading, when the diffusion is controlled by the collisions between sorbed molecules, neglecting lattice vibration has a strong effect on the diffusion dynamics, as it favors unphysical clustering and high-energy collisions, because of the lack of linear momentum conservation in sorbate motion.[19,72]

In conclusion, the inclusion of lattice vibrations is essential to provide in general a correct representation of the sorbate dynamics.

However, to assess the goodness of this approximation in this peculiar case, an obvious test can be the "experimental

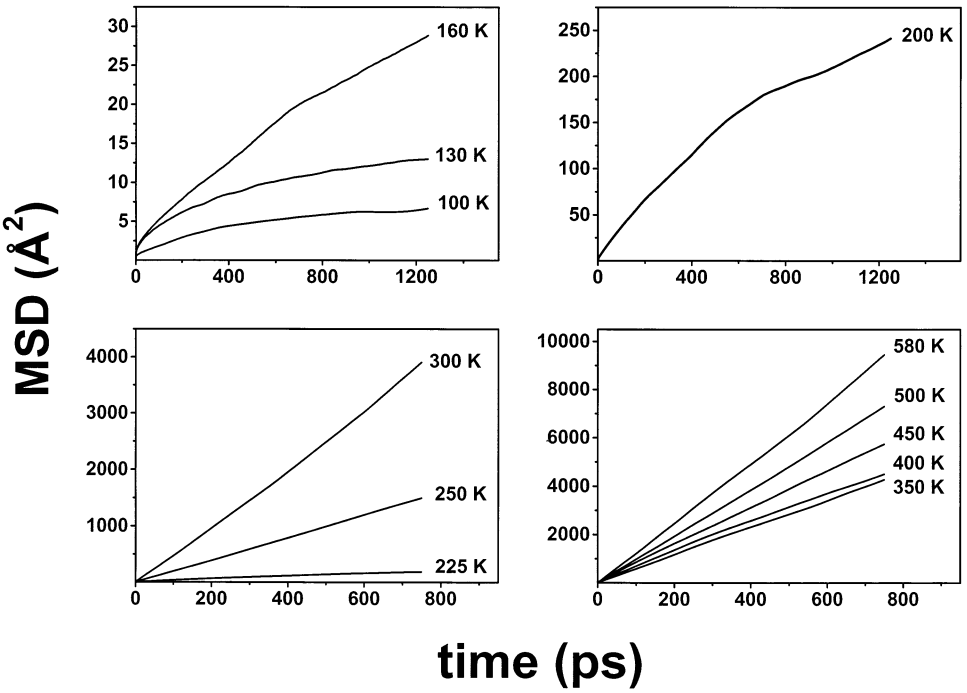

Figure 2. Mean square displacements of center of mass of water molecules in silicalite as a function of time, at different temperatures.

proof", which is the direct comparison of the results in the two cases, using the same potential model. Therefore, a test was performed using the model adopted in this work and keeping the framework fixed. The simulation was carried out assuming the experimental orthorhombic structure[11] at four different temperatures (240, 290, 320, and 400 K), allowing the comparison with the previous simulations and an estimate of the activation energy to diffusion. The resulting diffusion coefficient (see Figure 1) at 240 K is $1.27 \pm 0.13 \times 10^{-9}$ m^2 s^{-1}, at room temperature (290 K) is significantly different from the one obtained with the flexible framework ($8.5 \pm 0.9 \times 10^{-9}$ m^2 s^{-1}) and *smaller* (contrary to the results for methane, which yielded larger values for the fixed framework[58,69,72]) and at 320 K is $6.6 \pm 0.7 \times 10^{-9}$ m^2 s^{-1}, always smaller than the one evaluated with the flexible framework. On the contrary, at 400 K, the computed diffusion coefficient is *larger* than the one resulting from the flexible framework model ($1.50 \pm 0.15 \times 10^{-8}$ m^2 s^{-1} against $1.0 \pm 0.1 \times 10^{-8}$ m^2 s^{-1}). As it appears in Figure 1, the most striking difference between the fixed and flexible framework assumptions is that in the former case the activation energy is too high (both for the simulations of ref 20 and for ours), contrary to the experimental results, which yield an even slightly negative activation energy in the corresponding temperature range, whereas for the flexible framework model, the activation energy is almost constant. Also, the general trend is significantly different. In conclusion, in our opinion, the fixed framework approximation in this case does not hold satisfactorily, probably because, as for methane in silicalite (represented by a soft sphere),[58,69,72] during the collisions with the fixed framework the impulse is not conserved, entailing an unphysical strong backscattering. However, this extra backscattering, for a structured molecule like water, can be adsorbed in part by enhancing the intramolecular vibrations and rotational motions, which could hinder the diffusive process and therefore raise the activation energy to diffusion.

Another comparison with experiments can be made for the activation energy to diffusion. The experimental value in the range 280−400 K both for H- and Na-ZSM-5 is 16.5 kJ/mol, as evaluated from the data reported in ref 36, to be compared with the results of our simulations (see Figure 1) in the temperature range 225−300 K (where the Arrhenius plot is approximately linear) of 15.8 kJ/mol, a good agreement. This means that the barrier to diffusion is well reproduced by the adopted model, at least for temperatures below 300 K. In Na- and H-ZSM5, the barrier to diffusion persists for higher temperatures, probably because of the restricted available space. We remind that these values are not much different from the average experimental activation energy for bulk liquid water of about 20 kJ/mol, a value obtained from an approximate Arrhenius plot of the data reported in ref 73. A possible reason of the difference is that, in liquid water, each molecule makes with the surrounding ones on average about four hydrogen bonds (HB), which at each diffusive jump must be broken and restored, whereas in silicalite channels, the number of HBs is smaller. Indeed, an adsorbed water molecule cannot be completely surrounded by other ones, because of the too small available space.

Finally, the results of the ^{1}H NMR experiments, which suggest that water forms clusters below 265 K on the external surface of the crystallites or at the intersections between straight and sinusoidal channels,[30,31] may be compared with the simulated behavior of the adsorbed water. Indeed, below 200 K, the simulated water begins to form more and more stable clusters. However, we do not find that the number of HBs is on average greater than 3.5, as suggested by the experimentalists, because channel intersections are energetically unfavorable regions for water (see below and also the potential energy maps reported in ref 33). Moreover, on the basis of other experimental works on the phase transitions of nanoconfined water,[3−6] solidification in the channels should occur at temperatures much lower than 265 K, which is just below the freezing point of bulk water. Therefore, it is not sure that the clusters formed by the simulated water can be related with these experimental data.

Temperature Dependence of the Behavior of Water. Once it was ascertained that the simulation results matched reasonably the available experimental data and trends, the behavior of water outside the temperature range of experiments can be discussed.

TABLE 3: Computed Diffusion Coefficients and Their Components along Cartesian Axes (in 10^{-9} m^2 s^{-1}), δ and β Parameters [eqs 8 and 9, Respectively][a]

T (K)	D	D_x	D_y	D_z	δ	β
580	20.7	25.10	30.60	6.50	4.28	0.953
500	16.1	20.10	23.26	4.95	4.37	0.979
450	12.6	14.25	19.80	3.82	4.45	0.983
390	9.89	12.50	14.30	2.79	4.82	1.080
350	9.40	10.60	15.40	2.06	6.31	1.370
300	8.61	7.87	15.90	1.97	7.66	1.202
250	3.40	4.47	5.01	0.75	6.32	1.417
225	0.94	1.10	1.35	0.38	3.24	0.720

[a] The relative standard error of the computed values does not exceeds 10%.

The attention was focused first on the temperature dependence of MSD, which is displayed for different temperatures in Figure 2. A linear trend, corresponding to a normal diffusion, is observed for temperatures higher than 225 K. In Table 3, the computed diffusion coefficients are collected, and they are displayed in Figure 1 as an Arrhenius plot along with the results of experiments and other simulations. It is evident that the trend of the results of the present work is not a simple straight line, as for methane, but it is more complex. Above 350 K, the trend is linear, with an activation energy of about 5 kJ/mol; below 350 K, the slope diminishes abruptly, and a second linear interval corresponding to an activation of about 1 kJ/mol is observed down to room temperature. For lower temperatures, the curve is bent with negative curvature and becomes similar to the corresponding one for bulk liquid water, which is shown for comparison. As discussed above, the liquid water activation energy (and thus the average slope of the curve) is larger, because of the larger number of HBs that can be formed in liquid state. However, once this consideration is taken in account, the trend of the two curves appears very similar, and is characteristic of "fragile" liquids, where the energy landscape for the diffusing molecules changes strongly as the temperature changes. Indeed, as it is clear from Figure 3, the water−water potential energy rises from −15 to −3 kJ/mol in the temperature interval 220−580 K, whereas in the same interval, the water−framework energy variation (not shown) is almost linear and small (about 2 kJ/mol). Therefore, it is the change in the HB network and strength, which is crucial for explaining the observed trend. Possibly, the extension of the idea of fragile liquid to the extremely confined water in silicalite might be considered as speculative and hazardous, but the resemblance of the two curves is striking. Indeed, the computed values of the diffusion coefficients are nicely fitted by the well-known Vogel−Fulcher−Tamman equation,[74] which is currently used to represent the fragile liquid behavior

$$D = D_0 \exp[-E/R(T - T_0)] \tag{7}$$

where R is the gas constant and T is the temperature, and the fitted values of the parameters are $D_0 = 10.9 \times 10^{-9}$ m^2 s^{-1}, $E = 0.5155$ J mol^{-1} and $T_0 = 237.35$ K.

The data reported in Table 3 permit to discuss the anisotropy of the diffusion process. A simple random walk model,[75] derived for spherical adsorbed molecules, predicts that the diffusion coefficients along the straight channels D_y should be approximately twice the ones along the sinusoidal channels D_x, and they should be related to D_z, by the equation

$$\frac{a^2}{D_x} + \frac{b^2}{D_y} = \frac{c^2}{D_z} \tag{8}$$

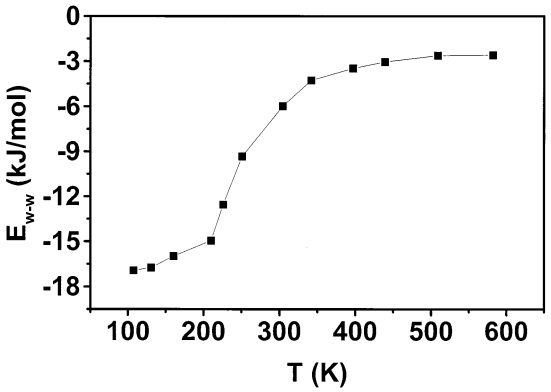

Figure 3. Intermolecular average potential energy of water in silicalite, as a function of temperature.

where a, b, and c are the unit cell dimensions. The discrepancy from this behavior is often measured by the parameter β, which is defined as[76−78]

$$\beta = \frac{c^2/D_z}{a^2/D_x + b^2/D_y} \tag{9}$$

If eq 8 holds, $\beta = 1$, whereas $\beta > 1$ means that the adsorbed molecules continue the diffusive motion preferentially along the same channel after crossing an intersection between straight and sinusoidal channels. Otherwise, for $\beta < 1$, the interchange between two crossing channels is the most probable event.

The values of β reported in Table 3 show that $\beta = 0.72 < 1$ at 225 K, but the mobility is very low and the value could be affected by statistical error. At higher temperatures, it becomes significantly greater than 1, reaching a maximum at 350 K ($\beta = 1.37$) and then it decreases and becomes close to 1 (within a few percent) in the temperature range 450−580 K. Our values are in partial agreement with the results of ref 38. The bias in molecular diffusion at intermediate temperatures depends probably on the molecular hydrogen bonded chains, which are formed in the channels and must bend to change the direction of motion at the intersections between channels. In practice, water clusters behave as the more tightly bonded molecules of alkanes, where $\beta = 1.3-1.4$.[77] At higher temperatures, the HBs are broken (see also below) and the molecular motion is randomized.

Another interesting parameter is the diffusion anisotropy, which is given by

$$\delta = \frac{1/2(D_x + D_y)}{D_z} \tag{10}$$

and following a random walk model should be $\delta \approx 4.4$.[75] Our simulations yield a value of δ close to the expected one only for the highest temperatures (greater than 450 K), at which the molecular motion is more randomized. At lower temperatures, D_z is lower than expected (see Table 3), in agreement with the trend to continue along straight or sinusoidal channels after crossing the intersections, given by $\beta > 1$ in the same temperature range. At 225 K, where $\beta < 1$, δ is less than expected.

As it appears in Figure 2, below 225 K the diffusivity is no more "normal", and the corresponding values of α [the exponent of time in eq 3] which are reported in Table 4, gradually lower, until they reach approximately the value $\alpha = 0.5$, characteristic of single-file diffusion. However, from the trends reported in Figure 2 only, it is not possible to understand the underlying

TABLE 4: Computed α Exponents Defined in eq 3, for the Total Diffusion and for the Diffusion along Cartesian Axes

T (K)	α	α_x	α_y	α_z
580	0.997	1.010	0.984	1.008
500	0.979	1.000	0.965	0.969
450	0.948	0.954	0.952	0.917
390	0.933	0.972	0.915	0.891
350	0.977	0.982	0.999	0.984
300	1.008	0.973	1.050	0.920
250	0.990	1.019	0.992	0.870
225	0.878	0.860	0.912	0.832
200	0.758	0.775	0.782	0.622
160	0.621	0.687	0.631	0.409
130	0.424	0.412	0.340	0.518
100	0.468	0.450	0.475	0.491

diffusive mechanism, and other quantities must be taken into account.

Another dynamical quantity which can be calculated from MD results, which can be evaluated by NMR spectroscopy, is the relaxation time τ_2 for the rotational motion of the water molecules. Following a well-established theory,[79] a quantitative comparison with NMR relaxation times is achieved by considering the second-order rotational correlation function

$$C_2(t) = \langle P_2[\mathbf{u}(0)\cdot\mathbf{u}(t)]\rangle \tag{11}$$

where $\mathbf{u}(t)$ is the versor of the HOH plane and P_2 is the second-order Legendre polynomial. Using eq 11, the relaxation time for rotational motion of water molecules τ_2 is evaluated by computing the time integral of $C_2(t)$

$$\tau_2 = \int_0^\infty C_2(t)\, \mathrm{d}t \tag{12}$$

The values of τ_2 were computed at room temperature, at 130 K, and at 580 K in order to estimate the activation energy for the rotational motion. Their values are 17.8 ps at 130 K, 0.06 ps at room temperature, and 0.03 ps at 580 K. Unfortunately, experimental measures for water in silicalite are not available, but the computed value at room temperature can be compared with the corresponding one in bulk water,[80] which is in the range 2.0−2.5 ps. The difference between τ_2 for water in silicalite and bulk water is large and can be interpreted as a signature of nearly free rotation, which is confirmed by the above-mentioned negligible computed activation energy. Moreover, the value of τ_2 was measured at 400 K for supercritical bulk water with a density ranging from 0.2 to 0.6 g cm^{-3}, a fluid which could be more similar to that of water in silicalite than ordinary bulk water.[81] The experimental results are in the range 0.03−0.06 ps, which are close to those of our calculations.

Diffusion Mechanism and Clustering of Adsorbed Water. To understand the microscopic behavior of molecules adsorbed in zeolites, a number of statistical tools can be applied to the raw simulation data.[19]

Let us consider first the radial distribution functions (rdf's) for the distances between the atoms of the sorbed molecules $g_{OO}(r)$ and $g_{OH}(r)$, which are reported in Figure 4. The other distribution function, $g_{HH}(r)$, will be neglected because it does not offer any interesting contribution in the following discussion. Although each molecule is not surrounded by other molecules as in bulk materials, these functions are useful to study the average intermolecular distances and the presence of hydrogen bonds.

At low temperatures, the rdf's show isolated peaks, indicating that all distances remain mostly around fixed values, a situation typical of stable clusters or solid state. The positions of first

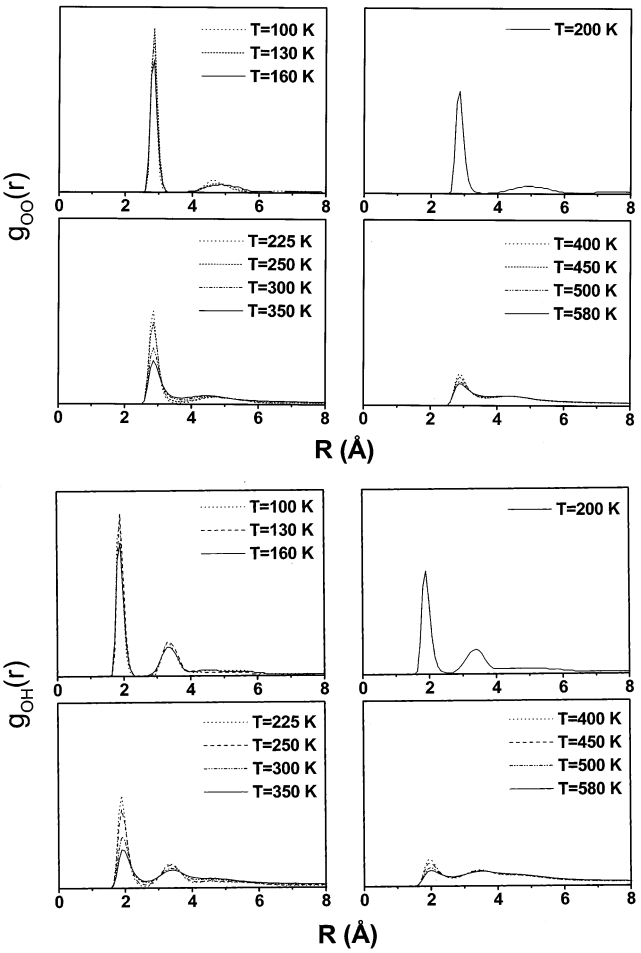

Figure 4. Intermolecular radial distribution functions of water molecules in silicalite, at different temperatures.

peaks in $g_{OO}(r)$ and $g_{OH}(r)$, which are located at about 0.28 and 0.19 nm, respectively, are a clear indication of the presence of stable hydrogen bonds. When temperature becomes higher than 225 K, the peaks begin to be connected, as it occurs in fluids, where interatomic distances can vary in a wide range of values. The maxima of $g_{OO}(r)$ and $g_{OH}(r)$ remain practically in the same positions, which means that the hydrogen bonds persist but can be less stable. At higher temperatures, the peaks broaden more and more, and finally, the second peak of $g_{OH}(r)$, at about 0.35 nm, becomes higher than the first one. This feature is apparent both in experimental (see for instance refs 82−84) and in Car-Parrinello simulations[85] of low-density supercritical water. Whether the water adsorbed in silicalite can be classified as a liquid or a vapor cannot be easily stated from the rdf's only. This problem can be discussed by considering, for instance, the temperature trend of average intermolecular energies (see Figure 3).

On the basis of the results reported in ref 49, we assume that in our model the energy of a hydrogen bond is about 8.5 kJ/mol, corresponding to the bonding energy of a water dimer per molecule. Therefore, it appears from Figure 3 at low temperatures (100−200 K) each water molecule forms at most about two HBs. By raising the temperature, the intermolecular energy gradually decreases, until, at 300 K, it becomes smaller than the HD bonding energy, indicating that, on average, stable HDs are no more present.

The three-dimensional distribution functions of the oxygen atoms in the channels, which are displayed in Figure 5, indicate that the molecules are constrained to remain around the channel

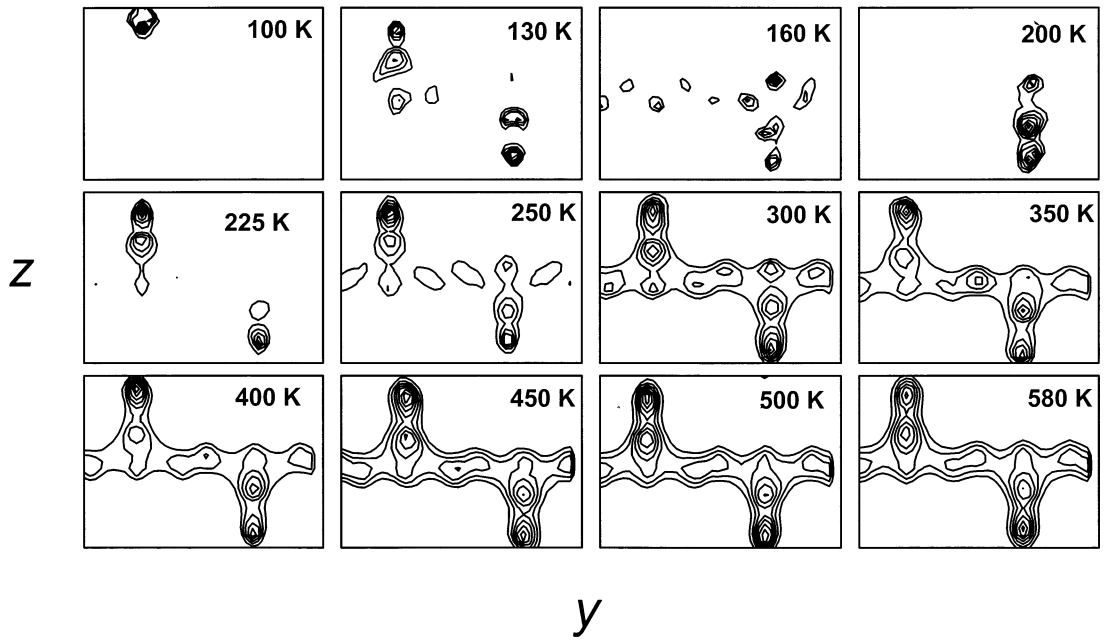

Figure 5. Contour plots of the density distribution function of the center of mass of water molecules in silicalite for the axial plane of the straight channel system, at different temperatures.

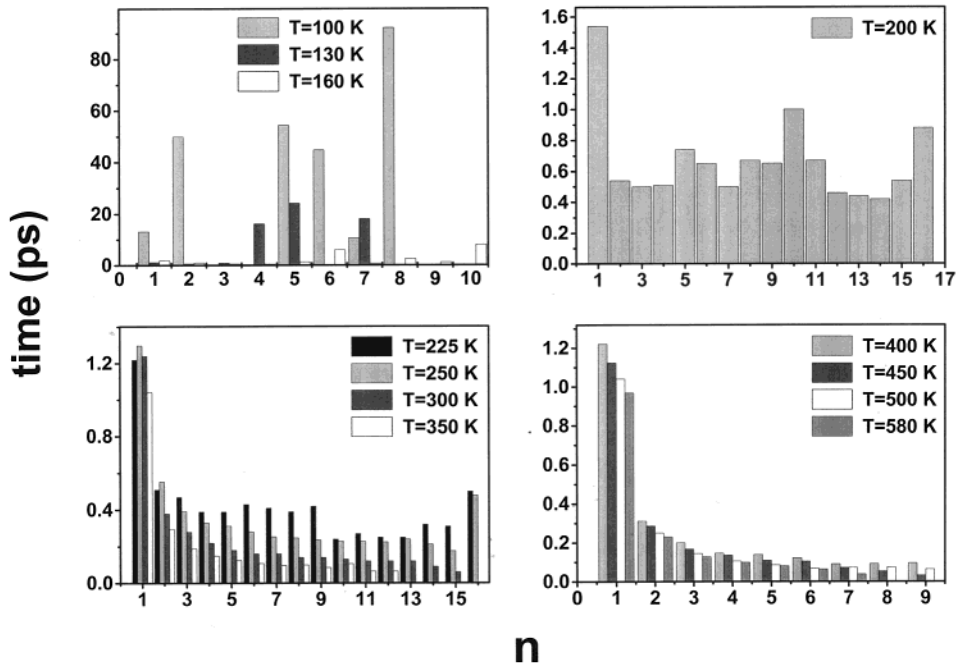

Figure 6. Mean lifetimes of water molecule clusters in silicalite, at different temperatures.

axes with relatively small oscillations of about 0.1 nm and that the intersections between channels are not preferred positions for the adsorbed molecules. Therefore, hydrogen bonded clusters can be present only in form of molecular chains, involving two HDs per molecule at low temperature, which is the same conclusion drawn on the basis of the intermolecular energies. Figure 5 shows that at low temperatures water molecules are localized around the potential energy minima, and the intermolecular distances measured at the oxygen atom locations are appropriate for HBs. Diffusive events are so rare that they do not contribute significantly to the distribution functions, and they appear as discontinuous.

Above 225 K, corresponding approximately to the onset of the "normal diffusion", the distribution functions become continuous and for temperatures higher than 300 K they are practically indistinguishable.

Another considered quantity which can help in understanding the diffusion mechanism is the mean lifetime of the adsorbed molecular clusters made of n molecules.[19,58] They are reported in Figure 6 and show a strong dependence on temperature.

For temperatures below 200 K, the lifetimes of the clusters are relatively large, though decreasing from almost 100 ps at 100 K to some picoseconds at 160 K. The most long-lived ones are those formed by 4−10 molecules, without a definite dependence on temperature. This irregular trend probably would disappear for simulations orders of magnitude longer than those actually obtainable. Indeed, we checked this possibility by repeating the simulation at 130 K by using an annealing

procedure as equilibration run: the distribution of the lifetimes of the clusters changed, although maintaining approximately the average duration of the lifetimes. Therefore, even from simulations of some nanoseconds, it appears that the clusters are not permanent and that an interchange of molecules occurs among them. This mechanism can explain the low but evident diffusivity shown by the MSD trends in Figure 2. Indeed, if the diffusion occurs through an exchange of molecules between wormlike clusters, which are nested in the channels (see for instance the distributions reported in Figure 5), only their ends are affected by the diffusive process and this is single-file like, with $\alpha \approx 0.5$ at 100 K, as reported in Table 4**.** Possibly, it might be suggested that a similar mechanism would describe the diffusivity in amorphous solid water,[43] where the mobility could rise near defective interfaces between small crystallites or nanoclusters similar to those found in silicalite but extended in three dimensions.

By raising the temperature, the mobility of the water molecules begins to grow along the sinusoidal channels first and gradually the diffusion mechanism approaches the "normal" one. Between 200 and 225 K, the lifetime of the clusters suddenly diminishes, becoming on average shorter than one picosecond, but more interestingly, the lifetime of clusters made of any number of molecules becomes approximately the same. This can be a signature of the "melting" of the clusters, as the molecules begin to move around and aggregate, forming hydrogen bonded "droplets" of continuously changing dimensions and thus of similar lifetimes. Indeed, as above-reported, the activation energy to diffusion in the range 225−300 K is about 16 kJ/mol, corresponding to breaking of two hydrogen bonds, which is just the number expected for a molecule belonging to a wormlike droplet contained in the narrow channel of silicalite. Moreover, the lifetimes of the clusters are approximately 0.5 ps in duration, which is close the lifetime of a single hydrogen bond in bulk liquid water at room temperature.[86] In conclusion, these arguments strongly suggest that the simulated water behaves as a liquid in the temperature range 225−300 K. The temperature of 200 K is a transition temperature, where $\alpha = 0.75$, a value just midway between "normal" and single-file diffusion, and the mean lifetimes of the clusters are nearly the same, but the distribution functions seem to be discontinuous.

At 300 K, the cluster lifetime distribution changes again. The trend vs *n*, the number of molecules contained in a cluster, becomes roughly exponential. The lifetime of the monomer is practically the same above 300 K (about 1.2 ps), but the lifetime of the clusters decreases for larger *n* more rapidly than for increasing temperature. This trend can be ascribed to a vaporlike state, as it is the same as for methane in silicalite at room temperature,[47] which is certainly a gas. The difference is in the value of the lifetime of the monomer, which is about three times the value for methane. This is reasonable, taking into account the smaller diffusivity of the water molecules as compared with the corresponding ones for methane, so that water molecules spend more time between collisions. Other simulation results support this conclusion: the lowering of the activation energy above 300 K, as a result of the lack of hydrogen bonds between the water molecules, entails an average intermolecular energy (see Figure 4) close or smaller than the thermal energy *RT* in this temperature range. Moreover, as remarked above, the relaxation time τ_2 for the rotational motion of the water molecules at room temperature is already of the same order of magnitude of the one at 580 K and of the experimental one for low-density supercritical water.

The existence of water in the vapor state in silicalite at room temperature was suggested by Giaya and Thompson in order to explain the results of experiments on adsorption of chlorinated hydrocarbons in silicalite where water was previously adsorbed[25] and was predicted by the same authors on the basis of an analytical model for the thermodynamics of water-like molecules contained in an infinite hydrophobic cylindrical channel.[9] Following this model, a vapor phase of adsorbed water is expected when the radius of the cylinder accessible to molecules is smaller than 0.2 nm. This is the case for water in silicalite, where it appears from the distributions shown in Figure 5 that this radius is somewhat smaller than 0.1 nm. It corresponds, always for the mentioned model, to a fluid−wall interaction energy slightly larger than 25 kJ/mol, which is close to our results (ca. 27 kJ/mol).

Some final general remarks could be added. Throughout this work, it is assumed that the simulated system follows the classical mechanics rules. This could be a good approximation if only translational and rotational motions were involved, like in fluids made by spherical or rigid particles. However, problems arise when classical molecular dynamics is applied to systems where vibrations are present, as for solids and structured molecules. Indeed, for these kind of systems, as observed in refs 19 and 87, to obtain the same vibration amplitude of an oscillator predicted by quantum mechanics, the total energy of a corresponding classical oscillator must include the quantum zero-point energy that in quantum systems does not enter in the evaluation of the temperature. As an example, it is shown in ref 87 that the average zero-point vibrational amplitude at about 0 K for the atoms of a zeolite framework corresponds to a classical temperature of about 400 K! Therefore, for zeolites simulated using classical MD, the vibrational amplitude of the framework atoms and of the water molecules is underestimated, and the available space to diffusion is larger than in the case of the more realistic quantum system. This could explain in part why the diffusivity resulting from the simulations is larger than the experimental one. On the other hand, the interactions between the framework and the diffusing molecules were optimized for the use of classical MD, and this fact could counterbalance in part the neglecting of quantum effects. The situation could be even worse if a first-principles method, as Car-Parrinello MD, would be used, because the motion of the nuclei follows classical mechanics, possible quantum corrections are not practicable for large systems, and the potentials, which are derived by quantum mechanical calculations, are not adjustable. Work is in progress to overcome this problem by avoiding a too heavy computational effort.

Conclusions

The computer simulation study illustrated in this paper demonstrates a complex behavior of water adsorbed in silicalite as temperature is changed. At low temperatures, it exhibits the properties of an amorphous solid with restricted but not completely frozen mobility, which could be explained as an exchange of single molecules between small clusters. At about 210 K, a temperature lower than the experimental limit of existence of supercooled water, as expected because of the very small dimensions of the adsorbing pores, the clusters "melt" and a liquidlike behavior is observed. The diffusion coefficients do not follow an Arrhenius trend, and the fluid behaves as a "fragile" liquid. Above about 300 K, again at a temperature lower than in the bulk, the confined fluid assumes some vaporlike characteristics, which are expected according to experimental and theoretical arguments.

How much these findings correspond quantitatively to the behavior of real water adsorbed in silicalite cannot be stated on the basis of the simulations only. However, the reproduction of the available experimental results at room temperature is, in our opinion, sufficiently good to attempt some qualitative conjectures about the diffusion mechanisms of water in silicalite at lower and higher temperatures.

Acknowledgment. This research is supported by Ministero dell'Istruzione, dell'Università, e della Ricerca (MIUR) by Università degli studi di Sassari and by Istituto Nazionle per la Scienza e Tecnologia dei Materiali (INSTM), which are acknowledged. We are grateful to Prof. Robert W. Thompson and Prof. Arjan Giaya for providing data before publication and for useful discussion. We are also indebted to Prof. Alberto Alberti for reading the manuscript.

Appendix

Analytical Form and Parameters of the Potentials for the Zeolite Framework. All of the charged particles interact via a Coulombic potential

$$V_C = \sum_{ij} \frac{q_i q_j}{4\pi\epsilon_0 r_{ij}} \qquad \text{(A1)}$$

where r_{ij} are the interatomic distances and q_i and q_j are the atomic charges whose values are ($e = 1.602 \times 10^{-19}$ C being the charge of one electron). For silicalite: $q_{Si} = 2e$ and $q_O = -1e$.

The potential for first-neighbors Si−O interactions is

$$V(r) = D\{1 - \exp[-\beta(r - R)]\}^2 - D \qquad \text{(A2)}$$

with the following values of the parameters:

$$D_{Si-O} = 648.52 \text{ kJ mol}^{-1}$$

$$\beta_{Si-O} = 0.97 \text{ Å}^{-1}$$

$$R(Si-O) = 1.875 \text{ Å}$$

The potential for interactions between the framework oxygen atoms of the same tetrahedron $V_{O-(T)-O}(r)$ and between the central atoms of adjacent tetrahedra $V_{Si-Si}(r)$ is

$$V(r) = V + 1/2k(r - R)^2 + 1/6A(r - R)^3 \quad \text{for } r < (R - 2k/A)$$
$$V(r) = 0 \quad \text{for } r < (R - 2k/A) \qquad \text{(A3)}$$

where

$$V_{O-(Si)-O} = -627.6 \text{ kJ mol}^{-1}$$

$$V_{Si-Si} = -1924.64 \text{ kJ mol}^{-1}$$

$$k_{O-(Si)-O} = 878.64 \text{ kJ mol}^{-1} \text{ Å}^{-2}$$

$$-k_{Si-Si} = 418.40 \text{ kJ mol}^{-1} \text{ Å}^{-2}$$

$$A_{O-(Si)-O} = -1556.448 \text{ kJ mol}^{-1} \text{ Å}^{-3}$$

$$A_{Si-Si} = -301.248 \text{ kJ mol}^{-1} \text{ Å}^{-3}$$

$$R_{O-(Si)-O} = 2.56 \text{ nm}$$

$$R_{Si-Si} = 2.85 \text{ nm}$$

References and Notes

(1) Ricci, M. A.; Rovere, M. *J. Phys. IV* **2000**, *10*, 187.
(2) Ricci, M. A.; Bruni, F.; Gallo, P.; Rovere, M.; Soper, A. K. *J. Phys.*: *Condens. Matter* **2000**, *12*, A345.
(3) Bergman, R.; Swenson, J. *Nature* (*London*) **2000**, *403*, 283.
(4) Bergman, R.; Swenson, J.; Börjesson, L.; Jacobsson, P. *J. Chem. Phys.* **2000**, *113*, 357.
(5) Swenson, J.; Bergman, R.; Howells, W. S. *J. Chem. Phys.* **2000**, *113*, 2873.
(6) Swenson, J.; Bergman, R.; Longeville, S. *J. Chem. Phys*. **2001**, *115*, 11299.
(7) Truskett, T. H.; Debenedetti, P. G.; Torquato, S. *J. Chem. Phys.* **2001**, *114*, 2401.
(8) Giaya, A.; Thompson, S. W. *J. Chem. Phys.* **2002**, *116*, 2565. Truskett, T. H.; Debenedetti, P. G.; Torquato, S. *J. Chem. Phys*. **2002**, *117*, 8162. Giaya, A.; Thompson, S. W. *J. Chem. Phys.* **2002**, *117*, 8264.
(9) Giaya, A.; Thompson, S. W. *J. Chem. Phys.* **2002**, *117*, 3464.
(10) Koga, K. *J. Chem. Phys.* **2002**, *116*, 10882.
(11) Gallo, P.; Ricci, M. A.; Rovere, M. *J. Chem. Phys.* **2000**, *116*, 342.
(12) Demontis, P.; Suffritti, G. B.; Alberti, A.; Quartieri, S.; Fois, E. S.; Gamba, A. *Gazz. Chim. Ital*. **1986**, *116*, 459.
(13) Leherte, L.; Lie, G. C.; Swamy, K. N.; Clementi, E.; Derouane, E. G.; André, J. M. *Chem. Phys. Lett*. **1988**, *145*, 237.
(14) Leherte, L.; André, J. M.; Derouane, E. G.; Vercauteren, D. P. *Comput. Chem*. **1991**, *15*, 273.
(15) Leherte, L.; André, J. M.; Vercauteren, D. P.; Derouane, E. G. *J. Mol. Catal*. **1989**, *54*, 426.
(16) Leherte, L.; André, J. M.; Derouane, E. G.; Vercauteren, D. P. *Catal. Today* **1991**, *10*, 177.
(17) Leherte, L.; André, J. M.; Derouane, E. G.; Vercauteren, D. P. *J. Chem. Soc., Faraday Trans.* **1991**, *87*, 1959.
(18) Leherte, L.; André, J. M.; Derouane, E. G.; Vercauteren, D. P. *Int. J. Quantum Chem*. **1992**, *42*, 1291.
(19) Demontis, P.; Suffritti, G. B.*Chem. Rev.* **1997**, *97*, 2845.
(20) Faux, D. A.; Smith, W.; Forester, T. R. *J. Phys. Chem. B* **1997**, *101*, 1762.
(21) Faux, D. A. *J. Phys. Chem. B* **1998**, *102*, 10658.
(22) Faux, D. A. *J. Phys. Chem. B* **1999**, *103*, 7803.
(23) van Koningsveld, H.; Jansen, J. C.; van Bekkum, H. *Zeolites* **1990**, *10*, 235 and references therein.
(24) van Koningsveld, H. *Acta Crystallogr. B* **1990**, *46*, 731.
(25) Giaya, A.; Thompson, R. W.; Denkewicz, R. *Micropor. Mesopor. Mater*. **2000**, *40*, 205.
(26) Hummer, G.; Rasaiah, J. C.; Noworyta, J. P. *Nature* (*London*) **2001**, *414*, 188.
(27) Berezhkovskii, A.; Hummer, G. *Phys. Rev. Lett.* **2002**, *89*, 064503.
(28) Noon, W. H.; Ausman, K. D.; Smalley, R. E.; Ma, J. *Chem. Phys. Lett.* **2002**, *335*, 445.
(29) Gordillo, M. C.; Martí, J. *Chem. Phys. Lett.* **2001**, *341*, 250.
(30) Eroshenko, V.; Regis, R.-C.; Soulard, M.; Patarin, J. *C. R. Physique* **2002**, *3*, 111.
(31) Flaningen, E. M.; Bennett, J. M.; Grose, R. W.; Cohen, J. P.; Patton, R. L.; Kirchner, R. M.; Smith, J. V. *Nature* (*London*) **1978**, *271*, 512.
(32) Ison, A.; Gorte, R. J. *J. Catal.* **1984**, *89*, 159.
(33) Vigné-Maeder, F.; Auroux, A. *J. Phys. Chem.* **1990**, *94*, 316.
(34) Olson, D. H.; Haag, W. O.; Borghard, W. S. *Micropor. Mesopor. Mater.* **2000**, *35*−*36*, 435.
(35) Giaya, A.; Thompson, S. W. *Micropor. Mesopor. Mater*. **2002**, *55*, 265.
(36) Caro, J.; Hocevar, S.; Kärger, J.; Riekert, L. *Zeolites* **1986**, *6*, 213.
(37) Caro, J.; Bülow, M.; Richter-Mendau, J.; Kärger, J.; Hunger, M.; Freude, D.; Rees L. V. C. *J. Chem. Soc. Faraday Trans. 1* **1987**, *83*, 1843.
(38) Bussai, C.; Vasenkof, S.; Liu, H.; Böhlmann, W.; Fritzsche, S.; Hannongbuai, S.; Haberlandt, R.; Kärger, J. *Appl. Catal. A* **2002**, *232*, 59.
(39) Fritzsche, S.; Wolfsberg, M.; Haberlandt, R.; Demontis, P.; Suffritti, G. B.; Tilocca, A. *Chem. Phys. Lett.* **1998**, *296*, 253.
(40) Demontis, P.; Gulín González, J.; Suffritti, G. B.; Tilocca, A. *J. Am. Chem. Soc.* **2001**, *123*, 5069.
(41) Kopelevich, D. I.; Chang, H.-C. *J. Chem. Phys.* **2001**, *114*, 3776.
(42) Suffritti, G. B.; Demontis, P.; Ciccotti, G. *J. Chem. Phys.* **2003**, *118*, 3439.
(43) Smith, R. S.; Dohnálek, Z.; Kimmel, G. A.; Stevenson, K. P.; Kay, B. D. *Chem. Phys*. **2002**, *258*, 291.
(44) Debenedetti, P. G.; Stillinger, F. H. *Nature* (*London)* **2001**, *410*, 259.

(45) Angell, C. A. *Chem. Rev.* **2002**, *102*, 2627.
(46) Bussai, C.; Haberlandt, R.; Hannongbuai, S.; Jost, S. *Stud. Surf. Sci. Catal.* **2001**, *135*, 263.
(47) Bussai, C.; Hannongbuai, S.; Fritzsche, S.; Haberlandt, R. *Chem. Phys. Lett.* **2002**, *354*, 310.
(48) Bussai, C.; Hannongbuai, S.; Haberlandt, R. *J. Phys. Chem. B* **2001**, *105*, 3409.
(49) Cicu, P.; Demontis, P.; Spanu, S.; Suffritti, G. B.; Tilocca, A. *J. Chem. Phys*. **2000**, *112*, 8267.
(50) Stahl, K.; Kvick, Å.; Ghose, S. *Zeolites* **1989**, *9*, 303.
(51) Artioli, G.; Smith, J. V.; Kvick, Å. *Acta Crystallogr. C* **1984**, *40*, 1658.
(52) Kvick, Å; Stahl, K.; Smith, J. V. *Z. Kristallogr*. **1985**, *171*, 41.
(53) Demontis, P.; Suffritti, G. B.; Bordiga, S.; Buzzoni, R. *J. Chem Soc. Faraday Trans*. **1995**, *91*, 535.
(54) Wolf, D.; Keblinki, P.; Phillpot, S. R.; Eggebrecht, J. *J. Chem. Phys.* **1999**, *110*, 8254.
(55) Demontis, P.; Spanu, S.; Suffritti, G. B. *J. Chem. Phys*. **2001**, *112*, 8267.
(56) **)** Car, R.; Parrinello, M. *Phys. Rev. Lett.* **1985**, *55*, 2471.
(57) June, R. L.; Bell, A. T.; Theodorou, D. *J. Phys. Chem.* **1990**, *94*, 1508.
(58) Demontis, P.; Suffritti, G. B.; Fois, E. S.; Quartieri, S. *J. Phys. Chem.* **1990**, *94*, 4329.
(59) El Amrani, S.; Kolb, M. *J. Chem. Phys.* **1993**, *98*, 1509.
(60) Hahn, K.; Kärger, J. *J. Phys. Chem.* **1996**, *100*, 316.
(61) Keffer, D.; McCormick, A. V.; Davis, H. T. *Mol. Phys.* **1996**, *87*, 367.
(62) Mon, K. K.; Percus, J. K. *J. Chem. Phys.* **2002**, *117*, 2289.
(63) Pal, S.; Srinivas, G.; Bhattacharyya S.; Bagchi, B. *J. Chem. Phys.* **2002**, *116*, 5941.
(64) Turov, V. V.; Brei, V. V.; Khomenko K. N.; Leboda, R. *Micropor. Mesopor. Mater.* **1998**, *23*, 189.
(65) Turov, V. V.; Chodorowski, S.; Leboda, R.; Skubiszewska-Zieba, J.; Brei, V. V. *Colloids Surf. A* **1999**, *158*, 363.
(66) Jorgensen, W. L.; Chandrasekhar, J.; Madura, J. D.; Impey, R. W.; Klein, M. L. *J. Chem. Phys.* **1983**, *79*, 926.
(67) Krynicki, K.; Green C. D.; Sawyer, D. *Faraday Discuss. Chem. Soc.* **1978**, *66*, 199.
(68) Schüring, A.; Auerbach, S. M.; Fritzsche, S.; Haberlandt, R. *J. Chem. Phys.* **2002**, *116*, 10890.
(69) Demontis, P.; Suffritti, G. B.; Mura, P. *Chem. Phys. Lett.* **1992**, *191*, 553.
(70) Henson, F.; Cheetham, A. K.; Stockenhuber, M.; Lercher, J. A. *J. Chem. Soc., Faraday Trans.* **1998**, *94*, 3759.
(71) Jousse, F.; Vercauteren, D. P.; Auerbach, S. M., *J. Phys. Chem*. **2000**, *B 104*, 9768.
(72) Demontis, P.; Suffritti, G. B.; Fois, E. S.; Quartieri, S. *J. Phys. Chem*. **1992**, *96*, 1482.
(73) Price, W. S.; Ide, H.; Arata, Y. *J. Phys. Chem. A* **1999**, *103*, 448.
(74) Angell, C. A. *Science* **1995**, *267*, 1924.
(75) Kärger, J.; Ruthven, D. M. *Diffusion in Zeolites and Other Microporous Solids*; John Wiley & Sons: New York, 1992.
(76) Maginn, E. J.; Bell, A. T.; Theodorou, D. *J. Phys. Chem.* **1996**, *100*, 7155.
(77) Jost, S.; Bär, N. K.; Fritzsche, S.; Haberlandt, R.; Kärger, J. *J. Phys. Chem. B* **1998**, *102*, 6375.
(78) Kärger, J.; Demontis, P.; Suffritti, G. B.; Tilocca, A. *J. Chem. Phys*. **1999**, *110*, 1163.
(79) Gordon, R. G. In *Advances in Magnetic Resonance*; Waugh, J. S., Ed.; Academic Press: New York, 1968; p. 1−42, Vol. 3.
(80) Winkler, K.; Lindner, J.; Bürsing, H.; Vöhringer, P. *J. Chem. Phys*. **2000**, *113*, 4674.
(81) Matubayasi, N.; Nakao, N.; Nakahara, M. *J. Chem. Phys.* **2001**, *114*, 4107.
(82) Gobaty, Y. E.; Demianets, Y. N. *Chem. Phys. Lett.* **1983**, *100*, 450.
(83) Bellissent-Funel, M.-C.; Tassaing, T.; Zhao, H.; Giullot, B.; Giussani, Y. *J. Chem. Phys*. **1997**, *107*, 2942.
(84) Soper, A. K.; Bruni, F.; Ricci, M. A. *J. Chem. Phys.* **1997**, *106*, 247.
(85) Boero, M.; Terakura, K., Ikeshoji, T.; Liew, C. C.; Parrinello, M. *J. Chem. Phys.* **2001**, *115*, 2219.
(86) Monrose, C. J.; Bucaro, J. A.; Marshall-Coakley, J.; Litovitz, T. A. *J. Chem. Phys*. **1974**, *60*, 5035.
(87) Jobic, H.; Smirnov, K.; Bougeard, D. *Chem. Phys. Lett.* **2001**, *344*, 147.